NRC Research Press

ARTICLE

Ecosystem changes across a gradient of permafrost degradation in subarctic Québec (Tasiapik Valley, Nunavik, Canada)[1]

Maude Pelletier, Michel Allard, and Esther Levesque

Abstract: Permafrost thaw, tundra shrubification, and changes in snow cover properties are documented impacts of climate warming, particularly in subarctic regions where discontinuous permafrost is disappearing. To obtain some insight into those changes, permafrost, active layer thickness, vegetation, snow cover, ground temperature, soil profiles, and carbon content were surveyed in an integrated approach in six field plots along a chronosequence of permafrost thaw on an ice-rich silty soil. Historical air photographs and dendrochronology provided the chronological context. Comparison of the plots reveals a positive feedback effect between thaw settlement, increased snow cover thickness, shrub growth, increase in soil temperature, and the process of permafrost decay. By the end of the sequence permafrost was no longer sustainable. Along the estimated 90 year duration of the chronosequence, the originally centimeter-thin pedogenic horizons under mosses and lichens increased to a thickness of nearly 65 cm under shrubs and trees. Snow cover increased from negligible to over 2 m. The thickness of soil organic layers and soil organic matter content increased manyfold, likely a result of the increased productivity in the shrub-dominated landscape. The results of this study strongly suggest that permafrost ecosystems in the subarctic are being replaced under climate warming by shrub and forest ecosystems enriched in carbon on more evolved soils.

Key words: permafrost, subarctic, thermokarst, shrubification, snow cover.

Résumé : Le dégel du pergélisol, l'augmentation du couvert arbustif de la toundra (« shrubification ») et les changements de propriétés de la couverture de neige constituent des impacts déjà connus du réchauffement du climat, particulièrement dans les régions subarctiques où le pergélisol discontinu est en voie de disparition. Afin d'obtenir un aperçu de ces changements, le pergélisol, l'épaisseur de la couche active, la végétation, la couverture de neige, la température au sol, les profils de sol et le contenu en carbone ont été examinés selon une approche intégrée dans six parcelles de terrain dans une chronoséquence de dégel du pergélisol sur un sol limoneux riche en glace. Des photographies aériennes historiques et la dendrochronologie ont fourni le contexte chronologique. La comparaison des parcelles révèle un effet de rétroaction positive entre le tassement dû au dégel, la couverture de neige plus épaisse, la croissance d'arbustes, l'augmentation de la température du sol et le processus de dégradation du pergélisol. À la fin de la séquence, le pergélisol n'était plus durable. Au cours de la durée d'environ 90 années de la chronoséquence, les horizons pédogénétiques à l'origine minces de quelques centimètres sous la mousse et les lichens ont augmenté jusqu'à une épaisseur de presque 65 cm sous les arbustes et les arbres. La couverture de neige est passée de négligeable à une épaisseur

Received 11 October 2016. Accepted 3 September 2018.

M. Pelletier and M. Allard. Centre d'études nordiques, Université Laval, Québec, QC G1V 0A6, Canada.
E. Levesque. Université du Québec à Trois-Rivières, Trois-Rivières, QC G9A 5H7, Canada.
Corresponding author: Michel Allard (e-mail: michel.allard@cen.ulaval.ca).
[1]This article is part of a Special issue entitled "Arctic permafrost systems".

de plus de 2 m. L'épaisseur des couches organiques de sol et le contenu de matière organique du sol ont décuplé, probablement un résultat de la productivité accrue dans le paysage dominé par des arbustes. Les résultats de cette étude semblent clairement indiquer que les écosystèmes de pergélisol subarctiques sont remplacés, sous les effets du réchauffement du climat, par des écosystèmes d'arbustes et forestiers enrichis en carbone sur des sols plus évolués. [Traduit par la Rédaction]

Mots-dés : pergélisol, subarctique, thermokarst, augmentation du couvert arbustif, couverture de neige.

Introduction

Permafrost has been warming in most of the northern hemisphere over the 20th century and is reported to be degrading in many regions (Osterkamp and Romanovsky 1999; Romanovsky et al. 2010). Thermokarst is now transforming Arctic and subarctic landscapes and ecosystems are changing as the ground is affected by dynamic processes associated with the melting of ground ice (Rowland et al. 2010; Kokelj and Jorgenson 2013). The global science community has expressed concerns about the fate of the carbon pool frozen in the permafrost that may contribute to climate warming by the release of greenhouse gases, referred to as the permafrost carbon feedback (Schuur et al. 2015). However, carbon storage linked to uptake by increased primary production associated with vegetation shifts and soil organic matter accumulation in subarctic regions also needs to be better assessed. Field studies are necessary to observe those processes and to obtain quantitative parameters of utility for modellers.

In the discontinuous permafrost zone, under a given local climate regime, the thickness of the active layer and the spatial distribution of permafrost and unfrozen soils are controlled by topography and by the spatial variability of soil physical properties (grain size composition and thermal properties), surface hydrology, and vegetation and snow cover dynamics and thickness (Gold and Lachenbruch 1973). These factors govern the ground surface temperature regime at the site level (Zhang et al. 1996). In Nunavik (northern Québec), east of Hudson Bay, the decay of permafrost, or thermokarst, is very well documented in the discontinuous permafrost zone where palsas, peat plateaus, lithalsas, and permafrost plateaus are gradually disappearing. They are being replaced by thermokarst ponds and shrublands in depressed terrain (Allard and Seguin 1987; Buteau et al. 2004; Payette et al. 2004; Marchildon 2007; Fortier et al. 2008; Thibault and Payette 2009; Jolivel and Allard 2013). In fact, when early thermokarst initiates a depression in the terrain, water may pond and the depression may expand and develop into a thermokarst lake (Grosse et al. 2013). If no water is ponded, the hollow provides conditions favourable for shrub expansion. The depression, slight at the beginning, is colonized by shrubs that help capture wind-drifted snow (Roche and Allard 1996). It is also well documented that warming surface temperatures currently favour the expansion of shrub communities in the Arctic, leading to modifications of ground thermal regime and snow cover properties (Blok et al. 2011; Lawrence and Swenson 2011; Bonfils et al. 2012; Epstein et al. 2013). However, few field studies specifically assess the rate of change from one phase to the next in the transition from tundra on permafrost to shrubland and forest on non-permafrost conditions. In fact, there are very few systematic measurements of the changes in ground temperature regime and heat fluxes over the sequence of successive states that occur along the landscape evolution from permafrost to non-permafrost terrain.

Ground thermal properties determine the rate of heat exchange between the atmosphere and the soil as well as within the soil itself (Gold and Lachenbruch 1973; Farouki 1981; Allard and Seguin 1987). When the heat balance at the soil surface becomes positive,

permafrost degradation begins (Chouinard et al. 2007; Delisle 2007; Romanovsky et al. 2010). This balance depends not only on air temperature and solar radiation, but also on snow cover thickness, timing, and duration (Goodrich 1982; Roche and Allard 1996), which depends on precipitation, wind speed, topography, and vegetation structure (Ménard et al. 1998; Domine et al. 2011). Burial under snow can provide shelter for vegetation, protecting buds from desiccation and freezing during the winter because the snow cover is a buffer layer that reduces soil heat exchanges with cold winter air temperatures (Burn and Kokelj 2009). Several studies have documented the expansion of shrubs on the eastern coast of Hudson Bay (Gregoire and Begin 1993; Allard and Pollard 2011; Provencher-Nolet et al. 2014) and recent changes in regional vegetation composition and structure under recent warming (Myers-Smith et al. 2011; Ropars and Boudreau 2012; Tremblay et al. 2012). Greening and shrub expansion have also been reported throughout the North American Arctic region and beyond (Sturm et al. 2001; Elmendorf et al. 2012; Ju and Masek 2016). In permafrost regions, a thick snowpack can maintain the snow–ground interface temperature at a value near the freezing point throughout the winter (Goodrich 1982). If a depth hoar layer forms at the base of the snowpack, the basal temperature may be as high as 0.6 °C (Domine et al. 2011). In the coldest days of winter, soil surface temperatures can be as much as 30 °C warmer than the air temperature under the canopy of shrubs and snow (Myers-Smith et al. 2011). When the snow cover increases over years, the refreezing of the active layer is delayed, the zero curtain duration is extended, and cooling of the permafrost is slowed; eventually the thermal regime can evolve towards thawing conditions (Halliwell and Rouse 1989).

To our knowledge, no studies have yet measured the rates of environmental change that occurs during recent permafrost degradation and the changes that occur in the heat fluxes during the transition from permafrost to non-permafrost conditions. The primary objective of this study was to better characterize the phases of ecosystem change that accompany permafrost degradation. Specifically, we aimed to evaluate the changes in soil and the ground thermal regime associated with permafrost thaw, topographic settlement, change in snow cover depth, and the transition from tundra over permafrost to shrubland and forest over non-permafrost. Another aim was to determine the temperature changes that occurred in the solum (surface organic and subsurface mineral soil layers) and the related variations in soil carbon content. By studying changes in the site parameters along a landscape chronosequence representative of permafrost degradation, our study provides some quantification of the changes in heat and matter fluxes within and at the interface of the three layers of the permafrost-supported ecosystem: the vegetation/snow cover (or buffer layer), the active layer, and the permafrost (Vincent et al. 2017).

Context of the study site

The Tasiapik Valley (formerly called "Vallée-des-Trois") is located 6 km east of the village of Umiujaq on the eastern shore of Hudson Bay (Figs. 1A and 1B), in the discontinuous permafrost zone (Allard and Lemay 2012). The landscape contains an array of landforms, including tundra-covered permafrost mounds and plateaus, shrub-dominated shallow depressions, deep hollows, ravines, and thermokarst ponds (Seguin and Allard 1984; Allard et al. 1996; Delisle et al. 2003; Buteau et al. 2004; Calmels 2005; Calmels and Allard 2008; Calmels et al. 2008; Fortier and Aubé-Maurice 2008; Fortier et al. 2008). The vegetation in the valley is a mosaic of lichen tundra patches, shrub thickets, and forest stands (Marchildon 2007; Jolivel and Allard 2013; Provencher-Nolet et al. 2014), similar to the wider region (Lévesque et al. 1988). Surficial deposits in the valley consist of shell-rich gravelly ice-contact sediments, glacio-fluvial sand and gravels, gravelly raised beaches, nearshore marine-deposited sands, and deeper water sediments such as silt, with radiocarbon dates ranging from the inception of the Tyrrell Sea at the time of deglaciation 8000 years ago to

Fig. 1. (A) Location of Umiujaq, Nunavik (QC). (B) The study site located in the Tasiapik Valley near Umiujaq. Note location of nearby reference site VDTsb (background image from UMI-Orthomosaic 2010 and MTQ-09401, Government of Québec in Arc-GIS). (C) Location of the central point of the six sampling plots of the permafrost plateau (directly under numbers; photograph by second author). (D) Geometrical configuration of the circular survey plots (5 m diameter) with auger sites, organic/moss layers measurements, and soil moisture measurements along radii.

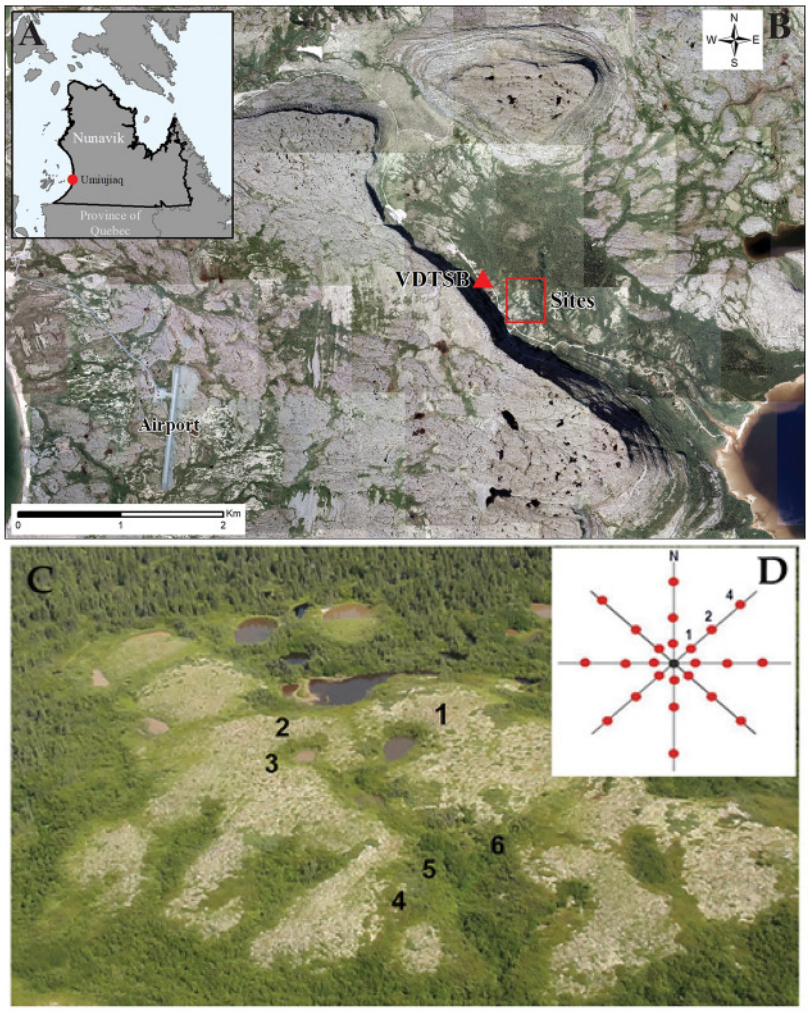

the postglacial sea during the Late Holocene (Lavoie et al. 2012). The postglacial marine limit is at 271 m a.s.l. Some organic sediments also occur in fens that have developed more recently in hollows and on poorly drained terrain (Ménard et al. 1998). The expansion of permafrost and the formation of segregated ice lenses in emerged fine-grained marine sediments during Late Holocene cold climate periods, between 2300 and 1800 BP, 1500 and 1000 BP, and during the Little Ice Age (Allard et al. 1987; Marchildon 2007) induced differential heave responsible for the formation of lithalsas and permafrost plateaus in the region (Ménard et al. 1998; Calmels 2005; Larrivée 2007; Calmels and Allard 2008; Fortier et al. 2008). This epigenetic permafrost contains almost no carbon or organic matter from marine sources (less than 1.25% loss on ignition; Calmels et al. 2008).

Air temperature data from the SILA-VDT (for Vallée-des-Trois) built by the Centre d'études nordiques in 2000 near the study site, and extended with reconstructed temperature data from the North American Regional Reanalysis database since 1979, revealed an average increase of 0.195 °C/year of mean annual air temperature (MAAT) from 1992 to 2012, for an absolute warming of 3.9 °C over 20 years, parallel to the regional trend shown by the Environment Canada meteorological station in Kuujjuarapik, 160 km south of the study area (Fig. 2A). Permafrost temperature recorded from a thermistor cable inserted in a permafrost mound (station VDTsb), located 270 m away from our study site and with the same geomorphology, clearly shows that the approximately 20 m thick permafrost warmed over that time and that thawing has occurred from both the top and the base of the permafrost (Fig. 2B). Gelifluction on the slopes of permafrost mounds and shallow landslides were observed during the period of active layer thickening (Seguin and Allard 1984). In brief, the ice-rich permafrost in this subarctic ecosystem has been degrading rapidly over the past decades with increasing air temperature, resulting in terrain subsidence and replacement of the tundra vegetation by erect shrub populations (Ropars and Boudreau 2012). Precise mapping of vegetation changes by Provencher-Nolet et al. (2014) in the Tasiapik Valley between 1994 and 2010, including and around our study site, showed an important increase in shrub cover (+12%) and a decrease in lichen cover (−8%). Similar changes were also mapped in the region by remote sensing by Beck et al. (2015) who also noticed a >10% increase in the normalized difference vegetation index over the study area from 1986 to 2009.

Methods

Field setup

First, a structural map of vegetation cover in the valley was interpreted from air photographs (UMI-Orthomosaic 2010 and MTQ-09401; resolution of 15 cm, obtained from the Government of Québec) with field checks. The structural classification scheme was modified from Payette and Gauthier (1972) by adding two additional plant strata to their original scheme: prostrate (0–0.1 m) and medium shrubs (0.5–1.5 m) (Pelletier 2015). One plot was then selected in each of six class units of the map (lichens, lichens and low shrubs, low shrubs and lichens, medium shrubs, high shrubs, and low trees) (Fig. 3 and Supplementary Fig. S1[2]). The six plots were selected on top and on the margins of a 4–5 m high permafrost plateau that had signs of thermokarst such as hollows and nascent ponds (Fig. 1C). The plots were circular around a central point with a radius of 5 m (78.5 m^2) (Fig. 1D). The stages of the chronosequence represented by the plots ranged from intact permafrost covered by lichen tundra at plot 1 to the absence of permafrost under trees at plot 6, with the intermediate plots showing progressively higher and denser shrubs, more subsided terrain, steeper slopes, and potentially thicker snow cover. All sites were situated on postglacial marine silt; thus, the thawing and settlement processes would be the same across the chronosequence. Therefore, the soil profiles across all the plots shared a single parent material with the same thermal and mechanical properties. This soil material is widespread in the postglacial marine overlap region of the postglacial Tyrrell Sea in the Hudson Bay region and is commonly associated with palsas, lithalsas, and thermokarst features, providing some regional significance to our process study (Allard and Seguin 1987).

[2]Supplementary material is available with the article through the journal Web site at http://nrcresearchpress.com/doi/suppl/10.1139/as-2016-0049.

Fig. 2. (A) Air temperature trends at Kuujjuarapik and Umiujaq for the period of 1925–2015 and 1977–2013 according to Environment Canada, SILA-Umiujaq weather station (CEN), and NARR data (North American Regional Reanalysis). (B) Mean annual permafrost temperature (MAGT) profiles at station VDTSB-2004, shown on two graphs for clarity. The first thermistor is 2 m deep. The year 2010 had the highest temperature on record so far. Note the increase of active layer depth and thawing at the base of the permafrost prior to 2008 and the rapid increase of active layer depth from 2008 to 2009 followed by a slight refreezing in 2011 and 2012.

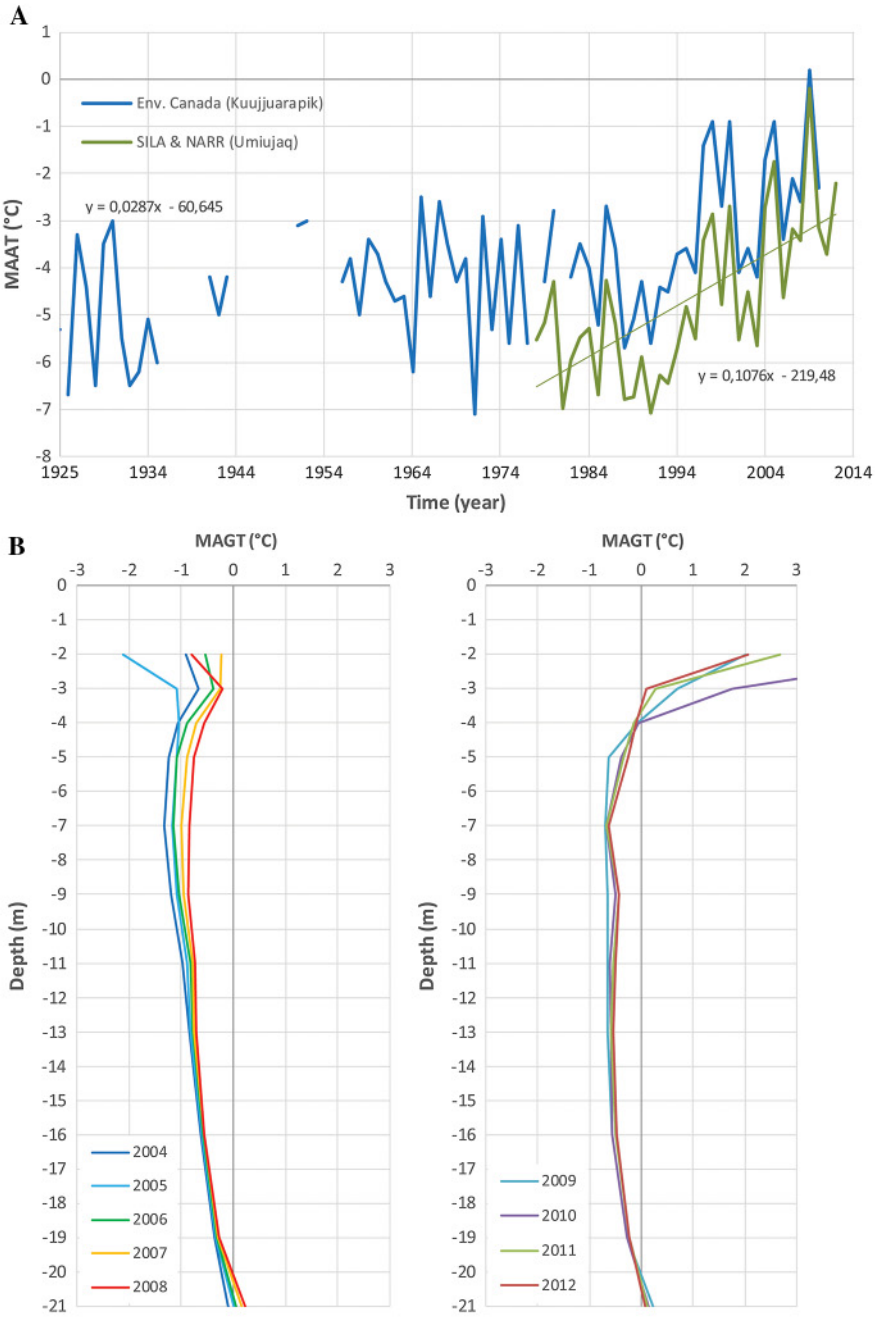

Fig. 3. Field view of the vegetation cover of the six study plots, Tasiapik Valley. See Fig. 4 and Table 2 for height and percent cover values.

In each plot, we characterized the permafrost (when present), measured the active layer thickness and properties, vegetation structure and composition (species), snow cover, organic cover, and pedogenic horizons. We also sampled carbon content in the form of soil organic matter. The near-surface soil temperature and moisture regime was also recorded for each plot. Chronology and rates of change in the ecological parameters between plots were assessed by using a combination of air photograph sequences and dendrochronology on stems and branches of shrubs and trees. For all parameters, the data acquisition approach followed the standardized Arctic Development and

Adaptation on Permafrost in Transition (ADAPT) project protocols (CEN 2014) (www.cen.ulaval.ca/adapt/protocols/adapt.php).

Local climate data

Climate data (temperature, precipitation, and wind) were obtained from two SILA Weather stations (Vallée-des-Trois (VDT) and Vallée-des-Trois, Sylvie Buteau (VDTsb), Tasiapik, Nunavik; Centre d'études nordiques (CEN), Université Laval, Québec (QC)), that had been in operation for nine years only a few hundred meters away from the study plots. The stations record data on an hourly basis, from which daily, monthly, and annual means, air thawing and freezing degree-days were calculated (see CEN 2018).

Permafrost

The nearby permafrost study site of Buteau et al. (2004) (VDTsb) was used as our benchmark for permafrost temperatures in near original conditions as the Centre d'études nordiques has maintained the thermistor cable that provides an excellent record of ground temperatures since 2002. The measurement accuracy is ±0.1 °C (L'Hérault 2009). As the permafrost at the study site and at the reference permafrost mound share the same morphology and geocryological composition, they also share the same thermal properties and regime.

Two continuous permafrost cores were extracted to a depth of 3 m with a portable drill at plots 1 and 2 (i.e., before or in the early stages of degradation) on 14 August 2013 (Calmels et al. 2005). The intact core increments were stored in plastic bags and sent frozen to Québec City. In the laboratory, the cores were subjected to CT imaging (Siemens Somatom Definition AS+ 128; resolution approximately 200 μm). Permafrost ice content in the form of pore ice (in pores >200 μm) and lenses, reticles, and veins was determined by pixel classification of the CT scan images following the methodology of Calmels and Allard (2008).

Active layer thickness and properties

Probing to the permafrost table was done with an open-face auger at plots 1–4. A 2 m long steel probe was also inserted into the ground to measure the depth to the top of the permafrost both by mechanical probing and by measuring temperature with a thermistor at the tip (permafrost having a temperature of 0 °C or less). At plots 5 and 6, no permafrost table could be reached mechanically because it was either too deep or non-existent. Temperatures were measured with the thermistor probe at every 25 cm to determine the thermal gradient within the active layer. The active layer depth was calculated by extrapolating the depth of the 0 °C isotherm on the temperature gradient.

Soil samples were extracted in short incremental sections using an open-face auger, kept in plastic bags, numbered, and the depth (cm) of the core sections was noted. The samples were taken to Laval University's laboratories for particle size analyses and water content determinations. Prior to particle size analysis, the organic matter was removed by ignition. Particle size distribution was determined by two methods: (1) sieving for the fraction >63 μm and (2) laser diffraction (with a Horiba particle size analyser) for the fraction <63 μm.

The microtopography within each plot was measured along eight, 5 m long, radial profiles along compass bearings (every 45°) from the central points of the plots (used as local reference) with a Zip-Level™ (Pro200 High Precision Altimeter, 0.2 mm precision). At the scale of the plots, the only conspicuous periglacial landforms were frostboils over permafrost.

Soil properties and carbon contents

At each plot, a pit was excavated in mid-August 2013 approximately 2 m from the plot center to describe soil horizons on a clean vertical cut approximately 80 cm deep.

The thicknesses of the organic layers, including the moss or litter layer, were measured. The mineral soil layers were also described based on color, organic matter content, and grain size composition. Each soil profile was photographed. The Canadian System of Soil Classification (3rd ed.; Agriculture and Agri-Food Canada 1998) was used as the reference. Volumetric cylinder samplers designed for the ADAPT project (101.76 cm^3) were inserted at five depths (litter/moss, −5, −15, −30, −60 cm, and at permafrost table depth) in the undisturbed active layer. This allowed for the measurement of bulk density. Total soil carbon and nitrogen contents were determined on each of the cylinder samples with a LECO C-H-N analyzer. The pH was measured on a pooled sample of six subsamples collected at the interface between organic and mineral horizons. To facilitate comparisons between various parameters (bulk density, C and N contents, and C/N ratios), two depth classes, 0–50 cm and 50–100 cm, were used during data processing and compilation. The upper section contained the organic horizons, whereas the lower section was mostly mineral, skeleton soil. Mean C and N concentrations (kg/m^3) were calculated for each layer. The total C and N storage and ratios for the complete active layer profile at each plot were obtained by adding the two layers together.

Soil temperature and moisture regime

At each plot, a small HOBO-Pendant™ datalogger (precision 0.53 °C) was installed at the ground surface (about 2–3 cm deep to avoid sun heating) under the dominant vegetation cover type to record hourly surface temperatures. Also, five thermal sensors (Decagon ECH20 5TE) were inserted in the canopy/snow cover at +20 cm (above surface), at the −5, −15, −30 cm depths, and at the permafrost table depth (or at least 1 m). Humidity and electrical conductivity sensors (Temp and Meter EC-5™ Soil Moisture Sensors) were inserted at 5 cm depth. In this study, the measured electrical conductivity was between 0.01 and 0.26 mmho/cm representing a range of 0.08–0.72 volumetric water content. The temperature sensors were calibrated to a precision of ±0.03 °C. The mean uncertainty obtained was 0.1 °C for all datalogger ports. The Decagon ECH20 dataloggers were run from 15 August 2012 to 16 August 2014. Temperature sensor data at +20 cm in the canopy of plot 2 contained many errors from 1 May 2013 onwards; those data were therefore discarded. Annual mean ground surface temperature (−5 cm), freezing (Fi) and thawing (Ti) indices, n-factors, and Fi/Ti ratios were calculated. Soil thermal conductivity values measured by Buteau et al. (2004) at the reference site were used to calculate the heat fluxes in the active layer. Those values were 2.6 W/(m·°C) for the frozen silty soil and 1.85 W/(m·°C) for the unfrozen soil. The standard equation for determining heat flux used was applied in the ground.

$$(1) \quad Q = k(T_1 - T_2)/(Z_1 - Z_2)$$

where Q is heat flux (W/m^2), k is soil thermal conductivity, T_1 and T_2 are temperatures (°C) at two given depths, and $Z_1 - Z_2$ is the depth interval (m). Results were comparable with those obtained by a fluxmeter plate on a silty soil near Manitounuk strait in Nunavik by Roche and Allard (1996).

Vegetation

During the field inventory, vegetation cover was described and quantified using Braun-Blanquet's (1932) cover-abundance method. The mean height and cover of each stratum of herb, shrubs, and tree species were measured in a 4 m^2 (2 m × 2 m) quadrat around the central point of each plot. Moss cover thickness was measured with a small ruler. Small samples (several grams) were taken in the surface 10 cm of soil for gravimetric water content determinations every meter along the radial transects (Fig. 1D).

Snow cover

During the first and second weeks of April 2013, at the time of maximum seasonal snow thickness, several snow pits were dug in the plots to gather information on snow cover stratigraphy, grain sizes, and shapes, using the "International classification for seasonal snow on the ground" as reference (Fierz et al. 2009). Snow density and temperatures were measured in the different snowpack layers. The snow thickness was probed randomly 10 times near the center of all plots. Snow water equivalent (SWE) was taken five times per plot with a standard Mount Rose sampler. The removed snow was put in plastic bags and weighted in a cold field laboratory in Umiujaq. Minimum, maximum, and mean values of the mass (kg) measurements were noted. SWEs (kg/m^2) were multiplied by the thickness of the snow samples collected to obtain bulk densities (kg/m^3). A set of two equations was used to determine the thermal conductivity and heat flux in the snow for the three plots that had significant snow covers (plots 4–6). The first equation by Sturm et al. (1997) was used to calculate the thermal conductivity according to snow density.

$$K_{\text{eff}} = 0.138 - 1.01\rho + 3.233\rho^2 \quad \text{for } 0.156 \leq \rho \leq 0.6 \tag{2}$$

where K_{eff} is the effective thermal conductivity (W/(m·°C)) and ρ is the snow density (in g/cm^3). The correlation between density and thermal conductivity is generally strong. However, this quadratic equation may yield erroneous values at the upper and lower end of the spectrum of densities. In this study, our measured snow density values fell in the middle of the possible spectrum of density.

Calculation of thaw settlement and thermokarst-related topographic change

The amount of thaw settlement (soil consolidation) that has occurred at the most degraded, subsided plots (4, 5, and 6) was estimated by multiplying the increment of active layer depth from one plot to the next (in cm) by the mean ice content (decimal fraction) averaged on the two permafrost cores (plots 1 and 2) taken together (for example, a 100 cm increase in active layer thickness and a 0.50 ice content will give a thaw settlement of 50 cm).

Chronology

To derive at least an approximate timing along the chronosequence of permafrost degradation, two complementary methods were used. First, five representative branches (birch, willow, and alder) or stems (black spruce) were collected near the ground in each plot and analysed by dendrochronology following standard procedures to provide minimum ages for establishment (Myers-Smith et al. 2015). Second, an enlargement of the National Air Photo Library 1:50000 air photograph of 1957 was obtained (made by blowing up the original negative film, giving a resolution of approximately 1 m) and visually compared with a large scale air photograph of 1994 and the high resolution satellite image of 2010. This time-lapse photographic approach provided a visual assessment of the expansion of shrubs and tree populations.

Results

The marine sediments consisted of clayey sandy silts (55% silt, 39% sand, 4% clay, and 3% gravel) (average of 47 samples). As observed in the cores extracted at plots 1 and 2, the ground ice in the permafrost consisted entirely of segregated ice lenses and veins making a reticulated cryostructure. Ice lens thickness varied from millimeters to centimeters. The biggest ice lenses were about 10 cm thick. Mean volumetric ice content in the permafrost to a depth of 2 m (61% and 37% at plots 1 and 2, respectively) provided a glimpse of the

spatial variability in the original ground ice distribution (Supplementary Fig. S2[2]). The layered cryostructure is almost identical to what was observed in the reference permafrost mound at VDTsb (Calmels and Allard 2008). The mean carbon content was about 0.1% at the base of the active layer (mean of 18 samples, range from 0.013% to 0.54%) and 0% in the permafrost.

It must be mentioned, however, that the rather high mean annual soil surface temperatures recorded in 2013 and 2014 at plots 1, 2, and 3 with a very thin snow cover (−0.4, −0.1, and 0.4 °C, respectively) are inconsistent with the presence of permafrost with such a shallow active layer as observed. Those values reflect the warm mean annual air temperatures in those years only and they reflect the fact the climate is variable and continues to get warmer in the region (Fig. 2A).

Even without a statistical analysis, the ranked sequence of most measured parameters was particularly clear from plots 1 to 5 (Table 1). Lichens, mosses, herbs, and woody growth forms changed from one plot to the next (Figs. 4A and 4B), whereas vegetation height and cover increased in steps from plots 3 to 4 and from plots 4 to 5. As selected in the field originally, topography ranged from slightly convex and flat to more depressed. The frost boils collapsed at plot 3 and they were no longer present at plot 4. Maximum thaw depth increased significantly between plots 3 and 4. The depth of pedogenic horizons were similar between plots 2 and 3, but it increased markedly from plot 4 onwards. The soil carbon content changed similarly. Summer surface temperatures were higher in plots 1 and 2. At plots 2 and 3, the thin snow cover had a minor dampening effect on the soil winter temperatures and only a slight surface cooling occurred under a deeper snow pack with a basal depth hoar layer at plot 4 (Figs. 5 and 6). In plots 5 and 6, the soil surface winter temperature was practically 0 °C and the permafrost table was >4 m or absent. This space for time sequence can be interpreted in terms of phases in the transition from permafrost to non-permafrost conditions, based on changes in the measured environmental variables (Table 1; see also Supplementary Fig. S3[2]).

Phases of permafrost degradation

Phase 0

The situation in plot 1 is taken as the starting phase (0), which corresponds to almost intact permafrost with only lichens and mosses and a few prostrate shrubs at the ground surface and bare frost boils (also supported by many years of past observations of similar settings in the region). During this phase, the ground surface temperature of thinly vegetated surfaces closely followed air temperature variations and in our plots the surface temperature ranged from −33 to 32 °C (see Plot 1; Fig. 5). The soil temperature regime was characterized by cold winter soil temperatures and large positive and negative heat fluxes in summer and winter, respectively (Figs. 5–7). The dominant prostrate shrubs included *Empetrum nigrum, Salix uva-ursi*, and*Vaccinium vitis-idaea* (Table 2). The herbaceous stratum was not very diverse and represented less than 3% cover. No or very thin organic layers were present at the surface of the frostboils, whereas depressions between the frostboils had relatively thick organic/moss layers with a high water content.

During this original phase, the permafrost table was almost 20 cm lower under the bare frostboils than under inter-frostboils covered by a thicker organic layer (Seguin and Allard 1984; Pelletier 2015). During strong wind periods, the snow was swept off the surface of the frostboils and carried into surrounding depressions, leaving the top of the plateau uncovered. The cryoturbation that operates in frost boils structured the cryosols, driven by humidity and heat conductivity contrasts between frostboils and inter-frostboils that create an annual convective cycle of differential frost heave and thaw settlement (Mackay 1980; Walker et al. 2004).

Table 1. Summary of observed features and measured key parameters of the permafrost ecosystem at the six plots.

Phase of permafrost degradation	~0	1		2	3	
Plot number	1	2	3	4	5	6
Landform	Slightly convex, frostboils	Slightly convex, frostboils	Flat, collapsing frostboils	Slightly depressed	Slope, depressed	Hollow
Vegetation	Lichens	Lichens and Low shrubs	Low shrubs and lichens	Low and medium shrubs	High shrubs	Low trees
Max. plant height (cm)	20	80	99	139	400	300
Moss/litter thickness (cm)	4	3	5	11	6	18
Snow cover depth (cm)	13	16	18	41	167	88
Mean snow cover density (kg/m^3)	154	163	168	288	349	239
Hoar layer thickness (cm)	—	—	—	45	55	48
ALT 2013 (cm)	133	124	125	202	420	—
MAST 2013–2014 (°C)	−0.4	−0.1	0.4	1.6	3.6	2.8
Maximum surface temperature 2013–2014 (°C)	32	20	16	14	14	15
Minimum surface temperature 2013–2014 (°C)	−33	−15	−20	−2	0	−2
n-factor, T	1.16	0.96	1.11	0.70	1.02	0.89
n-factor, F	0.66	0.52	0.52	0.13	0.00	0.05
Q_{min} 5–15 cm (W/m^2)	−0.4	−0.6	−0.5	−0.3	0.05	0.0
C content 0–1 m (kg/m^3)	3.0	6.4	8.8	38.3	39.4	22.9
C/N 0–50 cm	7.8	7.5	12.2	17.2	15.5	18.9
Duration (years)	ca. 400	ca. 23		ca. 10	ca. 23	>77
Timing	Before 1900	1957–1980		1980–1990	1990–2013	2013

Note: The two bottom lines of the table show the estimated duration of the phases and the approximate dates of transition between phases.

Fig. 4. Percentage vegetation cover at the six plots. (A) Mosses, lichens, and herbs. (B) Woody growth forms. Prostrate shrubs (0–0.1 m), low shrubs (0.1–0.5 m), medium shrubs (0.5–1.5 m), high shrubs (>1.5 m). Cover was assessed visually in 2 m^2 quadrats around the central points of the plots.

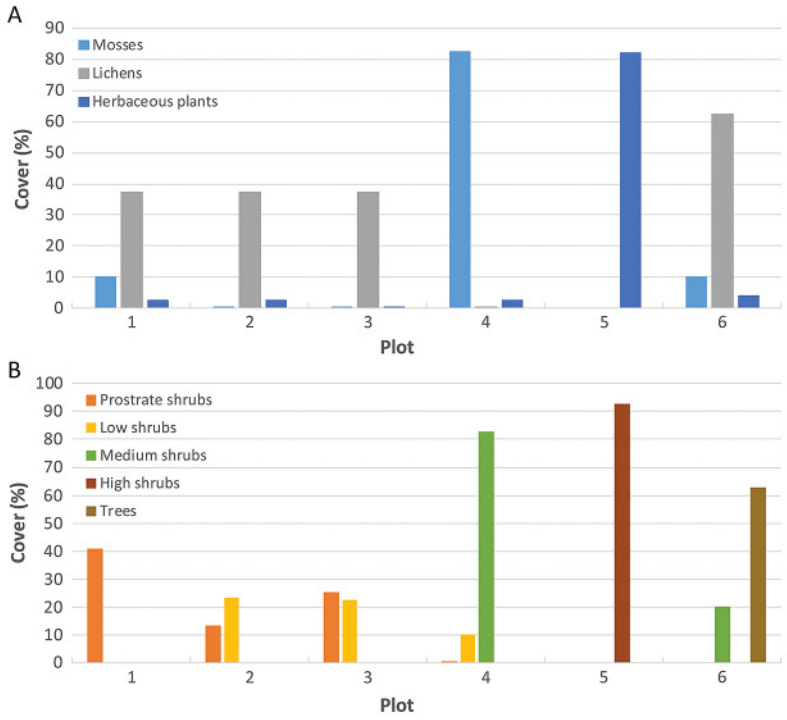

Phase 1

Phase 1, represented by plots 2 and 3, had slight permafrost degradation with lichens and a few prostrate shrubs rooted in micro-depressions between frost boils. *Empetrum nigrum* was the most abundant prostrate shrub species (Table 2). It is documented that this species increases in height and density with ground warming (Shevtsova et al. 1997; Alsos et al. 2007). Air temperatures were the main regulator of the ground thermal regime (Fig. 6). The snow cover increased only slightly in thickness during phase 1 but its density also increased due to wind compaction, so that its overall warming impact was slight. However, mean daily ground surface temperature (MDGT) fluctuations were reduced under erect shrubs. In our plots, the MDGT under the sparse cover of *Salix glauca* was reduced in summer and increased in winter, thus reducing the temperature amplitude to values between −20 and 15 °C under a 38 cm (plot 2) and 99 cm high cover (plot 3) (Fig. 5), likely by shading under small willows in summer and some dampening of cold air temperatures by the thin snow cover (about 18 cm). But overall mean surface temperatures remained about the same in these plots. By the end of phase 1, the frost boils became completely covered by mosses and other plants; the seasonal differential heave (cryoturbation) had slowed and the active layer must have started to deepen. A litter layer had begun to form, increasing the soil carbon content (Table 1). The depth of the pedogenic horizons was increased to about 25 cm in our plots. The increasing ground temperature, water content, and pedogenic activity allowed the growth of some species such as *Vaccinium vitis-idaea* (Table 2) (Shevtsova et al. 1997).

Fig. 5. Hourly mean ground surface temperature (−5 cm), recorded by micro data loggers from August 2012 to August 2013 under the dominant plant species in each plot.

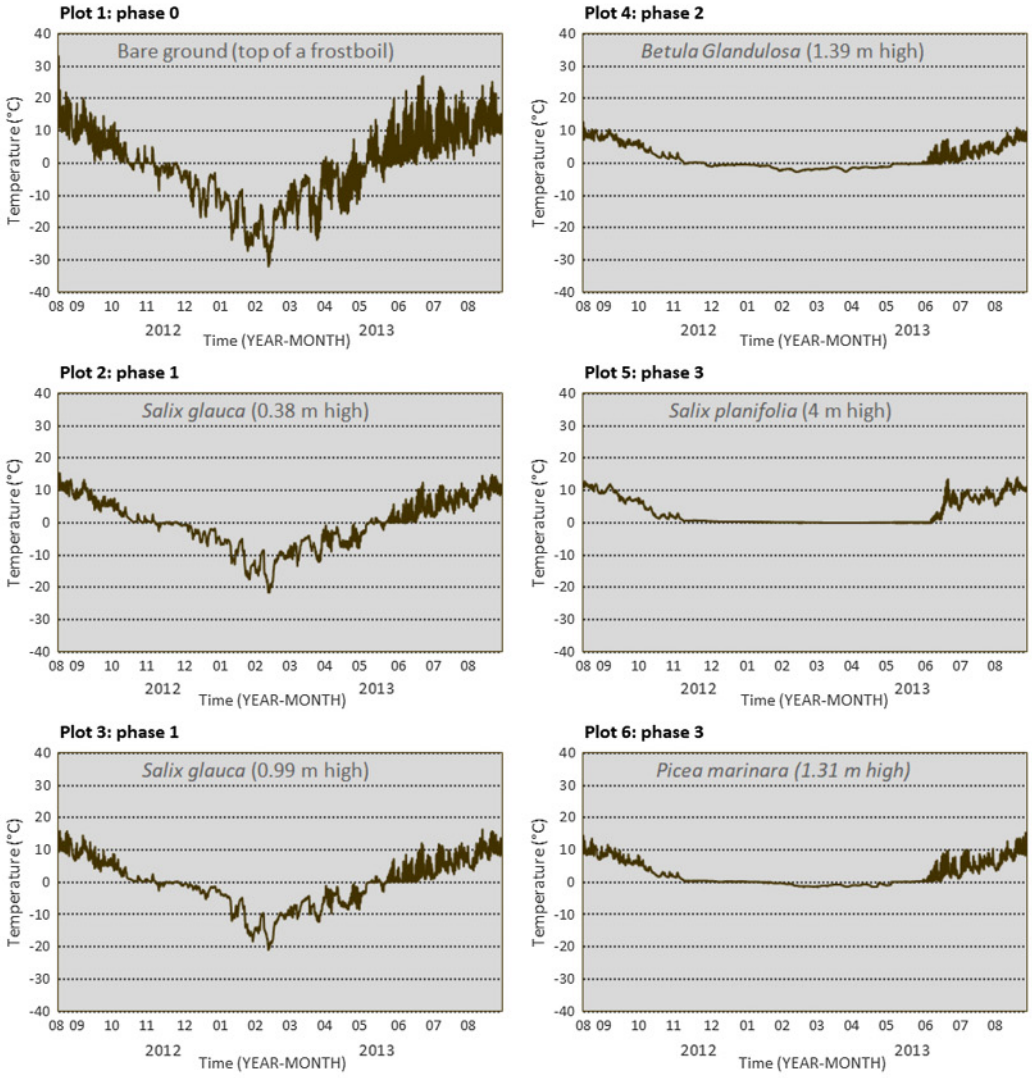

Phase 2

Phase 2 is represented by plot 4. Here, the low shrubs were replaced by higher ones. The increased cover of taller dwarf birch (*Betula glandulosa*) and willow (*Salix glauca*) (Fig. 4; Table 2) was likely favoured by snow accumulation in the slightly deeper topographic depression (Bret-Harte et al. 2001). The deepening of the topographic depression favoured the retention of more snow. The reduced temperature range of −2 to 14 °C under 139 cm tall *Betula glandulosa* resulted from the insulating effect of the thicker snow cover (Figs. 5 and 6). The increased snow cover depth and the intricate network of stems and branches changed snow cover properties. An important factor impacting the ground temperature regime was the formation of an insulating depth hoar layer at the base of the thick snow pack that greatly increased the surface offset through dramatic reduction of the freezing n-factor (Table 1) (Zhang et al. 1996). Soil temperature gradients and positive and negative heat fluxes were

Fig. 6. Relationship between daily air and ground surface temperatures at the six plots. Also indicated on the graphs are snow cover thickness (St) and mean annual ground surface temperature (MAGST).

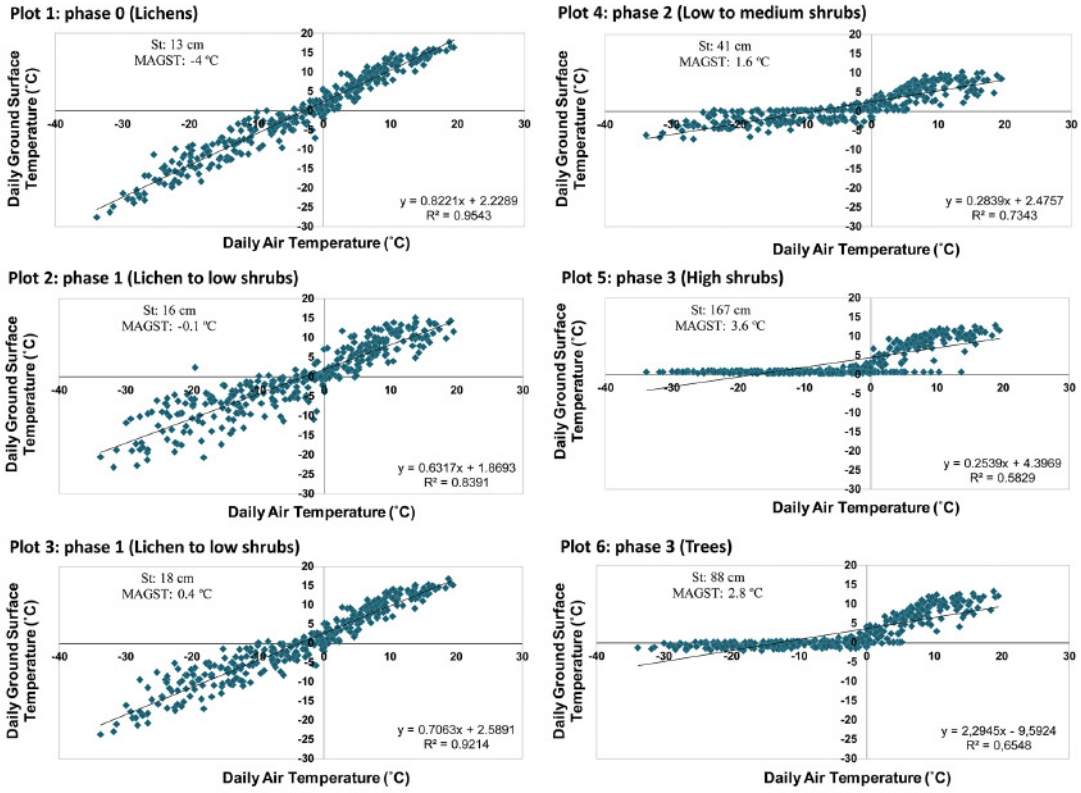

MAGST: Mean annual ground surface temperature
St: Mean snow cover thickness in April 2014

reduced given cooler temperatures under the canopy in summer and warmer soil temperatures in the active layer in winter (Fig. 7). The active layer depth increased and more ground settlement occurred. The deeper active layer and reduced amplitude of soil temperature and heat fluxes resulted in the loss of frost boils on the surface, although fossil traces of the cryoturbation could be seen in the soil horizons (see also Kokelj et al. 2007). The ground retained some moisture in summer, which further contributed to a change in the soil temperature regime to warmer conditions and favoured more shrub growth.

During phase 2, the greater shrub cover contributed to an increase in the thickness of the soil O horizons. The increasing snow cover thickness and thaw front depth favoured an increase in soil water content. Together, these soil conditions would have favoured nutrient uptake by microorganisms and deeper rooting plants (Chapin 1980; Chapin et al. 1995). It has been documented that certain shrub species, such as dwarf birch (*Betula glandulosa*), take advantage of increasing ground temperature and nitrogen availability for rapidly elongating shoots (Bret-Harte et al. 2001; Chapin et al. 2005; Buckeridge et al. 2010; Zamin and Grogan 2012).

Phase 3

In phase 3, which represents advanced permafrost degradation in the sequence, the vegetation becomes tall shrubs (plot 5) and small black spruce trees (plot 6). The near-surface

Fig. 7. Soil heat fluxes (*Q*) variations over one annual cycle (from August to August). *Q*1: (−5 to −15 cm), *Q*2: (−15 to −30 cm), *Q*3: (−30 cm to the depth of deepest thermistor). Positive values indicate a downward flux and negative values indicate upward flux.

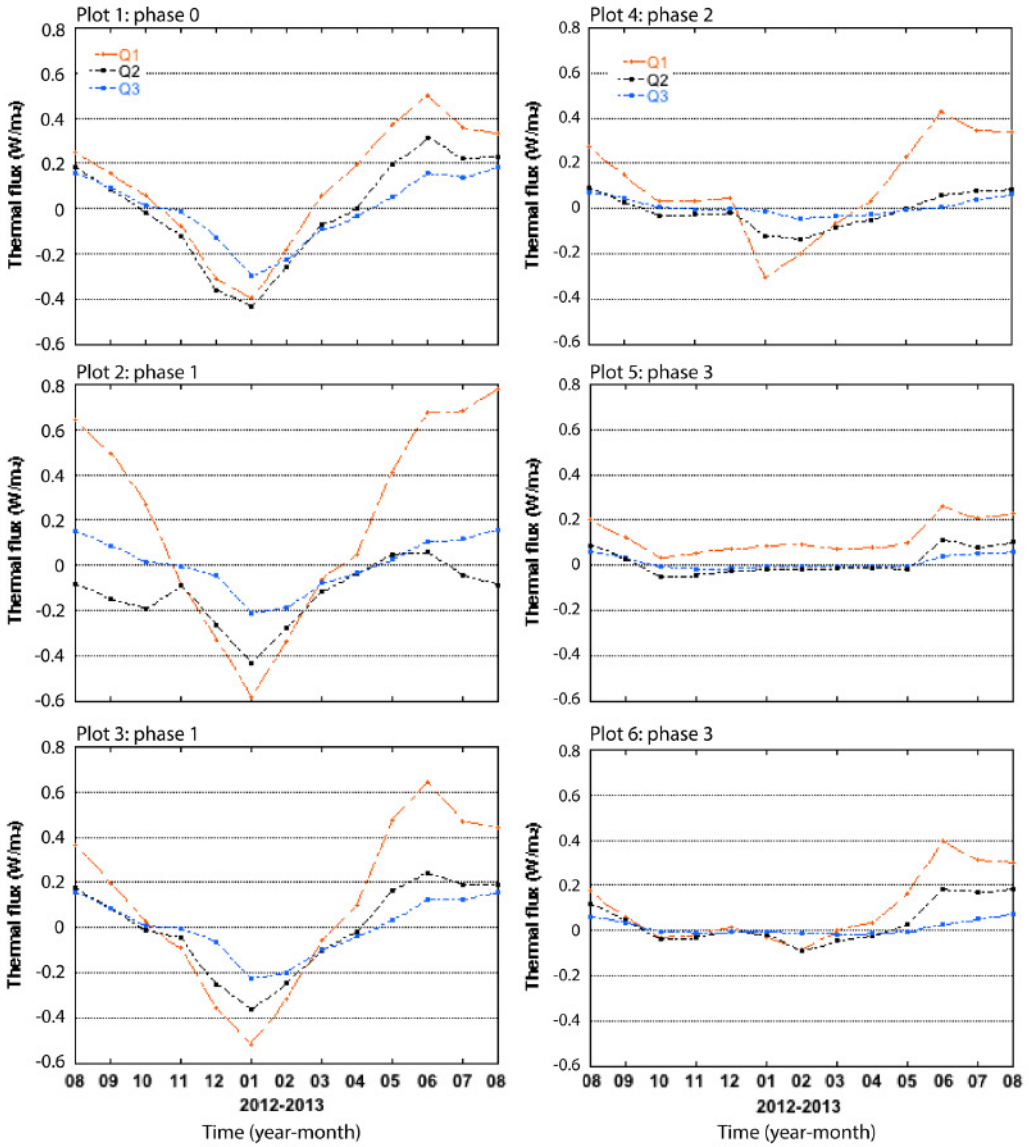

temperature amplitude was from −2 to 15 °C under the spruce stand (plot 6) and the temperatures stayed above the freezing point all year (0–14 °C) at plot 5 under the tall shrub cover. Either a supra-permafrost talik has developed or there is no more permafrost. At plot 5, not all soil water froze at the surface (−5 cm deep) and the near surface heat flux was even slightly positive in winter (Fig. 7) suggesting a small heat source beneath the snowpack, possibly due to some microbiological activity in the soil litter and in the organic horizons (Schimel et al. 2004; Sturm et al. 2005). Available moisture and more organic matter on the surface, supported by warmer temperatures, helped eluviation and the pedogenic profile reached a greater depth. Phase 3 represents advanced permafrost degradation

under tall shrubs and low trees (plots 5 and 6) when snow cover had reached a critical thickness and winter surface temperatures stayed close to 0 °C. This critical depth seems to be about 50 cm, as measured by Ménard et al. (1998), close to the value of 41 cm measured in plot 4. It may vary to some extent depending what fraction of it consists of the depth hoar layer (Zhang et al. 1996). The snow cover is thick and allowed the development of an approximately 50 cm thick depth hoar layer. A litter and/or a moss cover is present and the B horizons of the soil profile reach many decimeters in depth. At phase 3, the permafrost table reached deeper than 2 m, changing the soil order from a cryosol to a more evolved luvisol (Agriculture and Agri-Food Canada 1998).

Progression of environmental parameters and feedbacks during the chronosequence

The change from lichen tundra to low deciduous shrubs and, thereafter, to medium and high shrubs appears straightforward from phases 0 to 3 (i.e., from plots 1 to 5). However, it appears that phase 3 under trees at plot 6 is the end result of a different ecological pathway involving expansion of a pre-existing black spruce krummholz and, therefore had its own ecological history leading to permafrost degradation. In fact, *Picea mariana* was present on the permafrost plateau on the 1957 air photographs as sparse krummholz individuals in the tundra before the early phase of permafrost degradation. According to tree ring analyses, some spruce trees present today at plot 6 were already growing around 1913 (see below). Black spruce krummholz have been widely scattered in the shrub tundra biome for centuries. With climate warming, they now have the possibility to expand, start producing viable seeds, and be the core around which younger trees may grow in expanding forest stands (Payette et al. 1989).

The herbaceous stratum was not very diverse at the start of the chronosequence and it represented less than 2% cover in plots 1, 2, and 3, but it increased to 2.5% in plot 4 (phase 2). It further increased to 78% and became more diverse in phase 3 (plot 5) (Fig. 4; Table 2). Inversely, the prostrate shrub cover decreased in phase 2 (plot 4) (<1.0%) and no species of this stratum was found in plot 5. Plots with a low level of permafrost degradation (1, 2, and 3) had a high percent cover of prostrate shrubs (from 13% to 40.5%). Plots with more advanced permafrost degradation became dominated by stall shrubs to low trees. The composition of the shrub cover changed and *Salix glauca* increased in abundance from phases 1 to 2. *Salix planifolia* became dominant and was accompanied by *Alnus crispa* in phase 3 (Table 2).

On flat and convex surfaces corresponding to phases 0 and 1, the snow cover was very thin (plots 1, 2, and 3, maximum 18 cm), whereas on slopes and in depressions, the thickness became substantial after phase 2 (plots 4–6) (Table 1). At those advanced phases, interfaces between layers were sometimes very sharp, particularly at the top of the depth hoar layer (Supplementary Fig. S4[2]). The vertical heterogeneity within the snow pack increased with thickness. A few layers of rounded polycrystal snow grains were observed in the snowpack at plots 4–6, indicating accumulation of wind-drifted snow through the canopy in response to thaw settlement and shrub expansion (see also Roche and Allard 1996).

The soils in all plots were acidic with a pH between 4.7 and 3.8. A discontinuous layer of humus, less than 10 cm thick, was found in plots 1–3 (i.e., until the end of phase 1). The organic layer (Om) thickness increased from very thin to 10 and 20 cm at plots 4 and 6. Dead moss horizons changed to forest litter horizons, poorly decomposed materials changed to humic materials, and the top of mineral horizons became tinted by downward organic matter leaching, or eluviation, at plot 5. The thickness of the organic layer (moss and litter) increased progressively along the permafrost degradation/vegetation sequence.

Table 2. Percentage cover by plant species measured in quadrats at each plot.

Phase of permafrost degradation	0	1		2	3	
Plot number	1	2	3	4	5	6
Herbaceous species (%)						
Equisetum sp.	1	1	1	2	4	1
Carex sp.	0.5	0.5		0.5	—	0.5
Heracleum maximum	—	—	—	—	20	—
Solidago macrophylla	—	—	—	—	20	—
Rubus acaulis	—	—	—	—	37.5	—
Epilobium sp.	—	—	—	—	0.5	2.5
Prostrate shrub species (%)						
Empetrum nigrum	20	—	—	—	—	—
Vaccinium uliginosum	10	10	10	—	—	—
Vaccinium vitis-idaea	0.5	0.5	10	0.5	—	2.5
Salix uva-ursi	10	2.5	2.5	—	—	—
Ledum decumbens	—		2.5	—	—	—
Erect shrubs and trees (%)						
Betula glandulosa	—	2.5	2.5	10	—	—
Rhododendron groenlandicum	—	0.5	—	—	—	20
Salix glauca	—	20	20	82.5	—	—
Salix planifolia	—	—	—	—	82.5	—
Alnus crispa	—	—	—	—	10	—
Picea mariana	—	—	—	—	—	62.5

Soils on the permafrost plateau were *gleysolic turbic cryosols* (FAO-WRB equivalent: gleyic turbic cryosols) where cryoturbations were found in the organic (Om) and in the mineral (Bm, Bg, and Bh) horizons, with a gleyed C horizon immediately above the permafrost table. The B horizons appeared at phase 1 where uniform browning was observed. At phase 3 (plots 5 and 6), the profiles had evolved into *gleyed dark gray luvisols* (FAO-WRB: gleyic luvisols), with eluvial (Ae) and Bt horizons and degradation marks (h) (Supplementary Fig. S5[2]).

The carbon concentration in the top 50 cm increased correspondingly during phases 0 and 1 (2.7–5.9 and 8.3 kg/m^3 in plots 1–3, respectively) under lichens and prostrate shrubs and thereafter increased abruptly under low to medium shrubs in phase 2 (plot 4) (32.4 kg/m^3). Under high shrubs (plot 5) and low trees (plot 6), it decreased to 23.9 and 19 kg/m^3, respectively. At depths lower than 50 cm, the carbon content also increased throughout the sequence, albeit with lower values (0.2, 0.4, 0.4, 5.9, 15.6, and 3.9 kg/m^3 from plots 1 to 6, respectively). The summed carbon content in the pedogenic profiles shows a progressive increase throughout the permafrost degradation sequence (Table 1; Supplementary Fig. S6[2]).

To compare with other studies, our measured carbon concentration values (kg/m^3) were converted into soil organic carbon contents (SOC) (kg/m^2). The SOC of the active layer increased progressively during phase 1 (5.3, 11.2, and 15.4 kg/m^2) (plots 1–3, respectively). It quadrupled through phases 1–3 with respectively 67.0 and 68.9 kg/m^2 at plots 4 and 5. It is 40.1 kg/m^2 under the spruces at plot 6. Those values are consistent with those of Tarnocai et al. (2009) for the mean SOC of orthels (orthic turbic dystric cryosol) at about 4.5 kg/m^2 and at about 67.2 and 64.7 kg/m^2 for histels and histosols.

The thermal properties of the snow cover varied with structural vegetation growth forms. For the first three plots, the snow cover was too thin to induce a noticeable increase in the mean annual ground surface temperature. The overall thermal conductivity of the snow pack increased with thickness, although it increased mostly under high

shrubs (plot 5), where the mean value was 0.18 W/(m·°C), approximately 0.05 W/(m·°C) more than at other plots.

In Phases 2 and 3, the increased soil volumetric water content in the organic soil horizons delayed freeze-back in late fall under shrubs and low trees and in presence of a noticeable snow cover. This resulted in a long zero curtain period near the ground surface as happened at plots 4–6 (see Supplementary Fig. S7[2]). Unfrozen water content 5 cm deep in winter stayed at high values at plot 5 (above 0.2 m^3/m^3), compared with plots 4 and 6. At plots 4–6, late lying snow beds delayed the start of the soil thawing by 1 week, 1 month, and 2 weeks, respectively (Pelletier 2015). Both summer and winter soil heat fluxes were reduced and variability decreased with depth as shrubs got taller and snow depth increased with a depth hoar layer developing at the base (Fig. 7). In the high shrub phase 3 (plot 5), the ground surface heat flux stayed at a positive minimum of 0.05 W/m^2, increasing somewhat in the coldest months of the year. These positive, albeit small, values between −5 and −15 cm in winter indicate that there was a small downward heat flux from the soil surface under the snowpack in winter. In plots 5 and 6, the winter heat flux values near 0 W/m^2 in the deeper soil layers (Q2 and Q3) indicate there was no or very little heat loss from deeper horizons in phase 3 (Fig. 7).

The measured surface offset (i.e., difference between mean annual air temperature and soil surface temperature) increased strongly in the three last plots; it reached 1.4 °C in phase 2 and 1.7–1.8 °C in phase 3.

The increasing temperature at about permafrost table depth provoked permafrost thawing and ground surface settlements over the years. The permafrost table depth increased by 1.6 m from 2004 to 2012 at the reference thermistor cable (Fig. 2B). Given the average ground ice contents measured in the permafrost cores (approximately 49%), a settlement of about 0.4 m was calculated for the transition from phases 0 and 1 (plots 1–3) to phase 2 (plot 4). The settlement reached 1.45 m at phase 3 (plot 5). The disappearance of permafrost at plot 6 implies a much larger settlement of unmeasurable amplitude but likely on the order of 4.2 m, which is the approximate depth of the hollow relative to the permafrost plateau. However, it is also probable that a fraction of the total terrain settlement comes from thawing at the base of the permafrost, indicated by data from our reference thermistor cable (Fig. 2B), which shows that as permafrost becomes isothermal over its whole thickness, heat flow from beneath provokes also some basal thawing (Buteau et al. 2004).

Approximate dating and timing of the sequence

The mean ages of *Salix glauca* (plots 2–4) and *Salix planifolia* (plot 5) were between 15 and 20 years with an aging trend along the sequence. However, *Betula glandulosa* branches were older (30 ± 1.4 years old) at plot 4 where mean ages of *Salix planifolia* were about 20 years. At plot 6, the five stems of *Picea mariana* yielded a mean age of 77 years old (min 31, max 100). According to the aerial photographs, low shrubs were sparse at plot 4 and absent at plot 5 in 1957. A high density of low shrubs was visible on the photographs in 1994 at plot 4. In 2010, low shrubs (plot 4) and high shrubs (plot 5) and trees (plot 6) appear denser and taller than before on the photographs (Supplementary Fig. S8[2]).

Based on the data available (photo interpretation of images from 1957, 1994, and 2010) and the ages of woody plants, we deduced the approximate duration of the four phases backward from plot 5. The initial permafrost conditions (phase 0) date back to hundreds of years (i.e., since the formation of epigenetic permafrost in emerged marine sediments). Some prostrate shrubs were present at least for 37 years before a thermal impact could be felt on the ground. Phase 1, in response to rising air temperature, lasted approximately 23 years (plot 1 to the end of plot 3), roughly from 1957 to 1980. Phase 2 took approximately 10 years (ca. 1980–1990) (plot 4), and finally, phase 3 spanned about the last 23 years before

field work (plot 5) (Table 1). Given uncertainties resulting from the non-replication of the study plots in each phase, the limited number of permafrost cores, the limited frequency of aerial photographs, as well as the rather poor quality of available dendrochonological material, these time estimates of the permafrost degradation phases are only approximate. However, they are in agreement with observations reported in the literature and with human perception by local community members and berry pickers (Cuerrier et al. 2015; Gérin-Lajoie et al. 2016).

Discussion

Climate change and ecological feedbacks

Climate warming over the years was the initial cause of the observed changes by rising near-surface temperatures. At the core of this systemic evolution is the impact of shrub encroachment in tundra systems (Sturm et al. 2001; Sturm et al. 2005; Myers-Smith et al. 2011). The growth and expansion of low shrubs was first favoured and was gradually followed by medium and taller shrubs. Simultaneously, the permafrost warmed and the depth of thaw started to increase. Over time, the melting of the ground ice at the active layer/permafrost interface led to thaw settlement, creating depressions where thicker and denser snow could accumulate, in large part due to wind-drifting and trapping. Under the thicker snow cover, a depth hoar layer was formed. This favoured a sequence of permafrost thawing that evolved with continued warming and feedbacks, getting closer and closer to a threshold when site factors became the dominant drivers of change. The threshold was definitely exceeded when the mean winter soil surface temperature was 0 °C (Fig. 8).

Five main groups of environmental factors are involved in the sequence of permafrost disappearance: (1) atmospheric warming; (2) physical processes (change of vegetation structure, modification of snow cover properties (particularly the formation of a depth hoar layer), increase of unfrozen soil water content, ground ice melting, and thaw subsidence); (3) ecological processes (vegetation growth and succession and litter formation); (4) biogeochemical processes (build-up of pedogenic horizons, and carbon and nitrogen contents); all acting on (5), the soil thermal regime and the thawing of permafrost. The carbon cycle dynamics are also transformed through the transitional states of the ecosystem as the permafrost degrades. The abundant deciduous shrub cover is a storage compartment of carbon both above and below ground. The deciduous shrubs produce litter that decomposes to form organic soil layers that leach downward into the soil profile. From cryosols where the active layer had less than 1% carbon and a carbon-free mineral parent material at the start of the chronosequence, the soil in the plots with the deepest active layers and greatest shrub and tree covers (plots 4, 5, and 6) were significantly enriched in carbon. The increase in soil carbon and nitrogen availability likely promotes the further densification of shrubs (Sturm et al. 2005).

The warming climate, deepening of the active layer, biomass growth, thickening of litter and organic horizons, enrichment of the A horizon, deeper rooting depth, and the disappearance of permafrost are evidently making the ecosystem a carbon sink. Ecosystem changes associated with permafrost degradation, transition from tundra to forest and from cryosols to more developed soils shall likely build up an expanding carbon pool for many years to come (Mack et al. 2004; Davidson and Janssens 2006; Tarnocai and Stolbovoy 2006; Thompson et al. 2006). Ecosystem respiration and potential emission of CO_2 and CH_4 were not measured and subtracted in this study for an overall ecosystem balance, but the carbon balance at ground level is largely positive in the soil and the biomass.

Fig. 8. Flowchart model of the permafrost degradation chronosequence. In the left column the ground temperature regime is controlled by climate, principally air temperatures, as long as loop 1 is active, but loop 2 becomes gradually more important with increasing erect vegetation growth and snow cover thickness. When winter mean soil surface temperatures reach roughly 0 °C, the ground temperature regime shifts to site-controlled (right column); the ecosystem then evolves under loop 3 until the freezing depth does not reach the permafrost table anymore. A supra talik forms and permafrost either disappears or becomes relict.

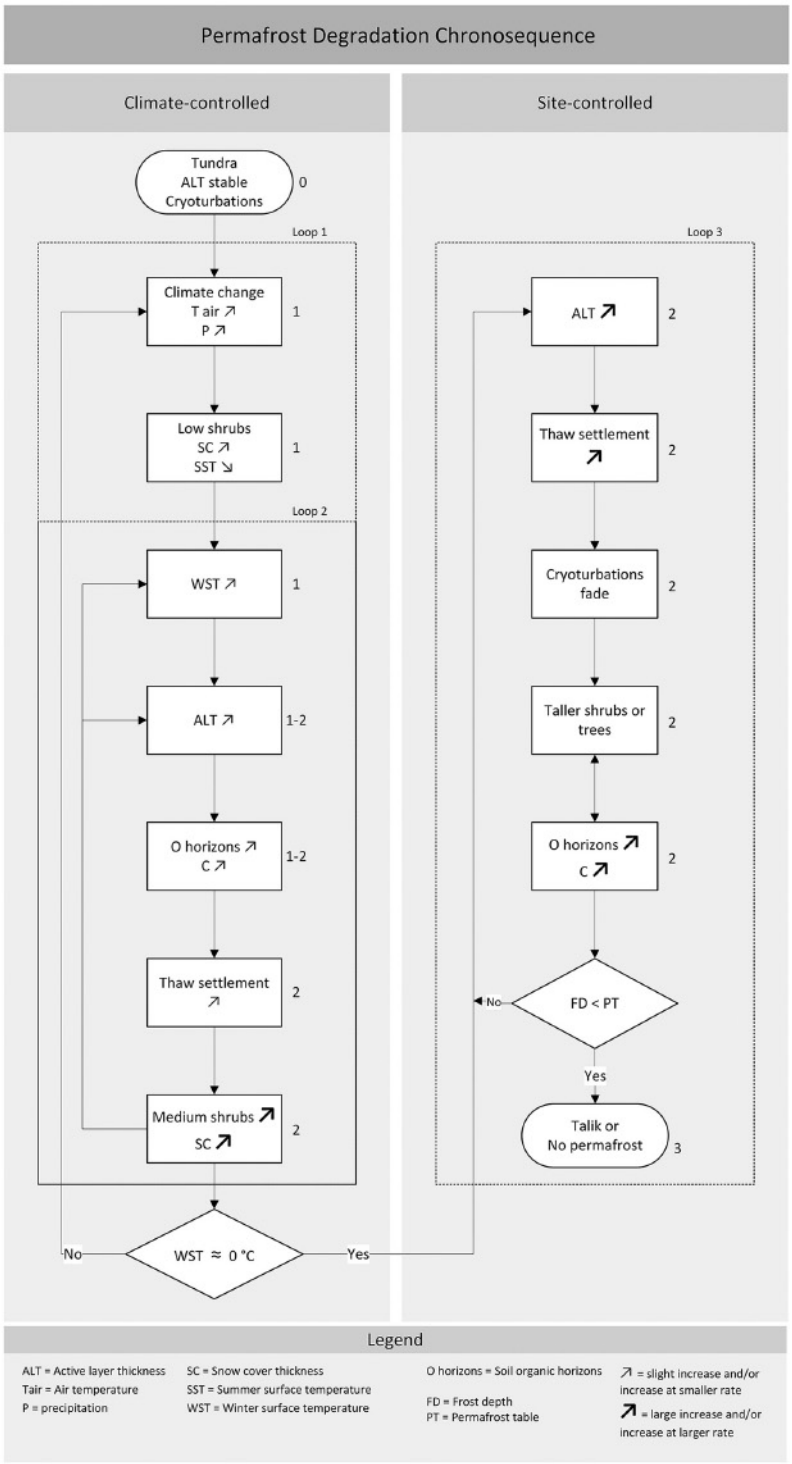

Conclusions

This research has helped to clarify the change of environmental conditions under which thawing proceeds over a silty ice-rich permafrost plateau in subarctic discontinuous permafrost. Based on our chronosequence, the rate of change of the physical and ecological variables was slow during the initial degradation phases of the permafrost when ground warming was primarily driven by slowly rising air temperature in the late 20th century, but it increased rapidly under continued warming once thaw settlement was initiated and the ground thermal regime became dominated by a thick snow cover accumulated in a progressively denser and higher shrub cover. The vegetation cover was transformed from lichens to shrubs or low trees with major shifts in structure and species composition. Annual mean temperatures at the snow–vegetation/ground interface increased from negative to about 0 °C. Positive winter heat fluxes in the first several centimeters of the ground even suggest a slight heat input explainable by a possible increase at some point in biogeochemical activity near the snow/soil interface. Overall, the soil in the transformed ecosystem has evolved into a greater organic matter sink.

The limited area of the study site based on a single (and highly thaw sensitive) soil parent material and under given climate conditions represents only a fraction of all the possible settings for processes and trends in the dynamic evolution of the three environmental layers of the permafrost system (vegetation/snow cover, active layer, and permafrost) across the Arctic regions. It would be useful to extend similar research approaches (with improvements) to other areas and other soil types to better document the ecological processes and impacts of permafrost degradation.

Acknowledgements

The authors sincerely thank the residents of the community of Umiujaq, for their friendly welcoming. We express our thanks to Dr. Martin Simard for his advice during the research. Thanks to all collaborators: Denis Sarrazin, Emmanuel L'Hérault, Andrée-Sylvie Carbonneau, Marilie Trudel, Catherine Jarry, Laurence Provencher-Nolet, Laurence Greffard, Jessica Leclerc, Joanie Tremblay, and Emmanuelle Vallières-Léveillé. This research was part of the Pan-Canadian Arctic Development and Adaptation to Permafrost (ADAPT) project. It also benefitted from support of various additional sources of funding: NSERC Discovery Grant to M. Allard, the ArcticNet network of centers of excellence and the EnviroNord scholarship program. We express our sincere thanks to Dr. Steve V. Kokelj, Dr. Juliane Wolter, the associate editor, and the editor of the Journal for the very helpful comments and suggestions made for improvements during the review process. The strong logistical support of Centre d'études nordiques (CEN) is also acknowledged.

References

Agriculture and Agri-Food Canada. 1998. The Canadian system of soil classification. 3rd ed. Soil Classification Working Group, Research Branch, Agriculture and Agri-Food Canada. NRC Research Press, Ottawa, Ont., Canada. Publication 1646. 187 pp.

Allard, M., and Lemay, M. (*Editors*). 2012. Nunavik and Nunatsiavut: from science to policy. An Integrated Regional Impact Study (IRIS) of climate change and modernization. ArcticNet Inc., Québec, Que., Canada. 303 pp.

Allard, M., and Pollard, W. 2011. Permafrost and climate change in Northern Coastal Canada. ArcticNet and Ouranos Project. Final Report. 19 pp.

Allard, M., and Seguin, M.K. 1987. The Holocene evolution of permafrost near the tree-line, on the eastern coast of Hudson Bay (northern Quebec). Can. J. Earth Sci. **24**: 2206–2222. doi: 10.1139/e87-209.

Allard, M., Seguin, M.K., and Lévesque, R. 1987. Palsas and mineral permafrost mounds in northern Québec. *In* International Geomorphology, 1986, Part II. *Edited by* V. Gardiner. Wiley & Sons, Chichester, New York. pp. 285–309.

Allard, M., Caron, S., and Bégin, Y. 1996. Climatic and ecological controls on ice segregation and thermokarst: the case history of a permafrost plateau in northern Quebec. Perm. Periglac. Proc. **7**(3): 207–227. doi: 10.1002/(SICI)1099-1530(199609)7:3<207::AID-PPP219>3.0.CO;2-4.

Alsos, I.G., Eidesen, P.B., Ehrich, D., Skrede, I., Westergaard, K., Jacobsen, G.H., Landvik, J.Y., Taberlet, P., and Brochmann, C. 2007. Frequent long-distance plant colonization in the changing Arctic. Science, **316**: 1606–1609. doi: 10.1126/science.1139178. PMID: 17569861.

Beck, I., Ludwig, R., Bernier, M., Lévesque, E., and Boike, J. 2015. Assessing permafrost degradation and land cover changes (1986–2009) using remote sensing data over Umiujaq, Sub-Arctic Québec. Perm. Periglac. Proc. **26**(2): 129–141. doi: 10.1002/ppp.1839.

Blok, D., Schaepman-Strub, G., Barholomeus, H., Heijmans, M.M.P.D., Maximov, T.C., and Berendse, F. 2011. The response of Arctic vegetation to the summer climate: relation between shrub cover, NDVI, surface albedo and temperature. Environ. Res. Lett. **6**: 035502. doi: 10.1088/1748-9326/6/3/035502.

Bonfils, C.J.W., Phillips, T.J., Lawrence, D.M., Cameron-Smith, P., Riley, W.J., and Subin, Z.M. 2012. On the influence of shrub height and expansion on northern high latitude climate. Environ. Res. Lett. **7**: 015503. doi: 10.1088/1748-9326/7/1/015503.

Braun-Blanquet, J. 1932. Plant sociology. The study of plant communities. McGraw-Hill Book Company, Inc., New York, N.Y., USA and London, UK. 439 pp.

Bret-Harte, M.S., Shaver, G.R., Zoerner, J.P., Johnstone, J.F., Wagner, J.L., Chavez, A.S., Gunkelman, R.F., IV, Lippert, S.C., and Laundre, J.A. 2001. Developmental plasticity allows Betula nana to dominate tundra subjected to an altered environment. Ecology, **82**: 18–32. doi: 10.2307/2680083.

Buckeridge, K.M., Zufelt, E., Chu, H., and Grogan, P. 2010. Soil nitrogen cycling rates in low arctic shrub tundra are enhanced by litter feedbacks. Plant Soil, **330**: 407–421. doi: 10.1007/s11104-009-0214-8.

Burn, C.R., and Kokelj, S.V. 2009. The environment and permafrost of the Mackenzie Delta area. Perm. Periglac. Proc. **20**(2): 83–105. doi: 10.1002/ppp.655.

Buteau, S., Fortier, R., Delisle, G., and Allard, M. 2004. Numerical simulation of the impacts of climate warming on a permafrost mound. Perm. Periglac. Proc. **15** (1): 41–57. doi: 10.1002/ppp.474.

Calmels, F. 2005. Genèse et structure du pergélisol: étude de formes périglaciaires de soulèvement au gel au Nunavik (Québec nordique), Canada. Ph.D. thesis, Université Laval, Québec, Que., Canada. 187 pp.

Calmels, F., and Allard, M. 2008. Segregated ice structures in various heaved permafrost landforms through CT Scan. Earth Surf. Process. Landforms, **33**: 209–225. doi: 10.1002/esp.1538.

Calmels, F.C., Gagnon, O., and Allard, M. 2005. A portable earth-drill system for permafrost studies. Perm. Periglac. Proc. **16**: 311–315. doi: 10.1002/ppp.529.

Calmels, F., Delisle, G., and Allard, M. 2008. Internal structure and the thermal and hydrological regime of a typical lithalsa: significance for permafrost growth and decay. Can. J. Earth Sci. **45**: 31–43. doi: 10.1139/e07-068.

CEN. 2014. ADAPT standard protocols. [Online]. Available from http://www.cen.ulaval.ca/adapt/protocols/adapt-fr.php.

CEN. 2018. Données des stations climatiques d'Umiujaq au Nunavik, Québec, Canada, version 1.5 (1997–2017). Nordicana, **D9**. doi: 10.5885/45120SL-067305A53E914AF0.

Chapin, F.S., III. 1980. The mineral nutrition of wild plants. Annu. Rev. Ecol. Syst. **11**: 233–260. doi: 10.1146/annurev.es.11.110180.001313.

Chapin, F.S., III, Shaver, G.R., Giblin, A.E., Nadelhoffer, K.J., and Laundre, J.A. 1995. Responses of arctic tundra to experimental and observed changes in climate. Ecology, **76**: 694–711. doi: 10.2307/1939337.

Chapin, F.S., Sturm, M., Serreze, M.C., McFadden, J.P., Key, J.R., Lloyd, A.H., and Welker, J.M. 2005. Role of land-surface changes in arctic summer warming. Science, **310**(5748): 657–660. doi: 10.1126/science.1117368. PMID: 16179434.

Chouinard, C., Fortier, R., and Mareschal, J.C. 2007. Recent climate variations in the subarctic inferred from three borehole temperature profiles in northern Quebec, Canada. Earth Planet. Sci. Lett. **263**(3): 355–369. doi: 10.1016/j.epsl.2007.09.017.

Cuerrier, A., Brunet, N.D., Gérin-Lajoie, J., Downing, A., and Lévesque, E. 2015. The study of Inuit knowledge of climate change in Nunavik, Quebec: a mixed methods approach. Hum. Ecol. **43**: 379–394. doi: 10.1007/s10745-015-9750-4.

Davidson, E.A., and Janssens, I.A. 2006. Temperature sensitivity of soil carbon decomposition and feedbacks to climate change. Nature, **440**: 165–173. doi: 10.1038/nature04514. PMID: 16525463.

Delisle, G. 2007. Near-surface permafrost degradation: how severe during the 21st century? Geophys. Res. Lett. **34**: L09503. doi: 10.1029/2007GL029323.

Delisle, G., Allard, M., Fortier, R., Calmels, F., and Larrivée, É. 2003. Umiujaq, northern Québec: innovative techniques to monitor the decay of a lithalsa in response to climate change. Perm. Periglac. Proc. **14**: 375–385. doi: 10.1002/ppp.469.

Domine, F., Bock, J., Morin, S., and Giraud, G. 2011. Linking the effective thermal conductivity of snow to its shear strength and density. J. Geophys. Res.: Earth Surf. **116**: F04027. doi: 10.1029/2011JF002000.

Elmendorf, S.C., Henry, G.H.R., Hollister, R.D., Björk, R.G., Boulanger-Lapointe, N., Cooper, E., Johannes, J., Cornelissen, H.C., Day, T.A., Dorrepaal, E., Elumeeva, T.G., Gill, M., Gould, W.A., Harte, J., Hik, D.S., Hofgaard, A., Johnson, D.R., Johnstone, J.F., Jónsdóttir, I.S., Jorgenson, J.C., Klanderud, K., Klein, J.A., Koh, S., Kudo, G., Lara, M., Lévesque, E., Magnússon, B., May, J.L., Mercado-Díaz, J.A., Michelsen, A., Molau, U., Myers-Smith, I.H., Oberbauer, S.F., Onipchenko, V.G., Rixen, C., Martin-Schmidt, N., Shaver, G.R., Spasojevic, M.J., Þórhallsdóttir, D.E., Tolvanen, A., Troxler, T., Tweedie, C.E., Villareal, S., Wahren, C.-H., Walker, X., Webber, P.J., Welker, J.M., and Wipf, S. 2012. Plot-scale evidence of tundra vegetation change and links to recent summer warming. Nat. Clim. Change, **2**: 453–457. doi: 10.1038/nclimate1465.

Epstein, H.E., Myers-Smith, I., and Walker, D.A. 2013. Recent dynamics of arctic and sub-arctic vegetation. Environ. Res. Lett. **8**(6): 15040. doi: 10.1088/1748-9326/8/1/015040.

Farouki, O.T. 1981. Thermal properties of soils. CRREL Monograph 81-1. Cold Regions Research and Engineering Laboratory, Hanover, N.H., USA. 151 pp.
Fierz, C., Armstrong, R.L., Durand, Y., Etchevers, P., Greene, E., McClung, D.M., Nishimura, K., Satyawali, P.K., and Sokratov, S.A. 2009. The international classification for seasonal snow on the ground. IHP-VII Technical Documents in Hydrology N°83, IACS Contribution N°1. UNESCO-IHP, Paris, France.
Fortier, R., and Aubé-Maurice, B. 2008. Fast permafrost degradation near Umiujaq in Nunavik (Canada) since 1957 assessed from time-lapse aerial and satellite photographs. *In* Proceedings of the 9th International Conference on Permafrost. Fairbanks, Alaska, USA, 29 June–3 July 2008. *Edited by* D.L. Kane and K.M. Hinkel. Institute of Northern Engineering, University of Alaska Fairbanks, Fairbanks, Alaska, USA. Vol. 1, pp. 457–462.
Fortier, R., Leblanc, A.-M., Allard, M., Buteau, S., and Calmels, F. 2008. Internal structure and conditions of permafrost mounds at Umiujaq in Nunavik, Canada, inferred from field investigation and electrical resistivity tomography. Can. J. Earth Sci. **45**(3): 367–387. doi: 10.1139/E08-004.
Gérin-Lajoie, J., Cuerrier, A., Siegwart Collier, L., and Collaborators. 2016. "Caribou taste different now". Inuit elders observe climate change. Arctic College in coll. with Inhabit Media, Baffin, Nun., Canada. Inuktitut and English. 314 pp.
Gold, L.W., and Lachenbruch, A.H. 1973. Thermal conditions in permafrost: a review of North American literature. *In* North American Contribution to the 2nd International Conference on Permafrost, Yakutsk, USSR. National Academy of Science, Washington, D.C., USA. pp. 3–25.
Goodrich, L.E. 1982. The influence of snow cover on the ground thermal regime. Can. Geotech. J. **19**(4): 421–432. doi: 10.1139/t82-047.
Gregoire, M., and Begin, Y. 1993. The recent development of a mixed shrub and conifer community on a rapidly emerging coast (Eastern Hudson Bay, subarctic Québec, Canada). J. Coastal Res. **9**: 924–933.
Grosse, G., Jones, B., and Arp, C. 2013. Thermokarst lakes, drainage, and drained basins. *In* Treatise on geomorphology. *Edited by* J.F. Shroder. Academic Press, San Diego, Calif., USA. pp. 325–353.
Halliwell, D.H., and Rouse, W.R. 1989. A comparison of sensible and latent heat flux calculations using the Bowen ratio and aerodynamic methods. J. Atmos. Ocean. Technol. **6**(4): 563–574. doi: 10.1175/1520-0426(1989)006<0563:ACOSAL>2.0.CO;2.
Jolivel, M., and Allard, M. 2013. Thermokarst and export of sediment and organic carbon in the Sheldrake River watershed, Nunavik, Canada. J. Geophys. Res.: Earth Surf. **118**: 1729–1745. doi: 10.1002/jgrf.20119.
Ju, J., and Masek, J.G. 2016. The vegetation greenness trend in Canada and US Alaska from 1984–2012 Landsat data. Remote Sens. Environ. **176**: 1–16. doi: 10.1016/j.rse.2016.01.001.
Kokelj, S.V., and Jorgenson, M.T. 2013. Advances in thermokarst research. Perm. Periglac. Proc. **24**: 108–119. doi: 10.1002/ppp.1779.
Kokelj, S.V., Burn, C.R., and Tarnocai, C. 2007. The structure and dynamics of earth hummocks in the subarctic forest near Inuvik, Northwest Territories, Canada. Arct. Antarct. Alp. Res. **39**: 99–109. doi: 10.1657/1523-0430(2007)39[99:TSADOE]2.0.CO;2.
Larrivée, E. 2007. Tomographie électromagnétique du pergélisol près d'Umiujaq, Nunavik (Québec). M.Sc. thesis, Université Laval, Québec, Que., Canada. 149 pp.
Lavoie, C., Allard, M., and Duhamel, D. 2012. Deglaciation landforms and C-14 chronology of the Lac Guillaume-Delisle area, eastern Hudson Bay: a report on field evidence. Geomorphology, **159–160**: 142–155. doi: 10.1016/j.geomorph.2012.03.015.
Lawrence, D.M., and Swenson, S.C. 2011. Permafrost response to increasing Arctic shrub abundance depends on the relative influence of shrubs on local soil cooling versus large-scale climate warming. Environ. Res. Lett. **6**: 045504. doi: 10.1088/1748-9326/6/4/045504.
Lévesque, R., Allard, M., and Seguin, M.K. 1988. Regional factors of permafrost distribution and thickness, Hudson Bay Coast, Québec, Canada. *In* Proceedings of Fifth International Permafrost Conference, August 2–5, Trondheim, Norway. *Edited by* K. Senneset. Vol. 1, pp. 199–204.
L'Hérault, E. 2009. Contexte climatique critique favorable au déclenchement de ruptures de mollisol dans la vallée de Salluit, Nunavik. M.Sc. thesis, Laval University, Department of Geography, Québec, Que., Canada. 129 pp.
Mack, M.C., Schuur, E.A.G., Bret-Harte, M.S., Shaver, G.R., and Chapin, F.S. 2004. Ecosystem carbon storage in arctic tundra reduced by long-term nutrient fertilization. Nature, **431**: 440–443. doi: 10.1038/nature02887. PMID: 15386009.
Mackay, J.R. 1980. The origin of hummocks, western Arctic coast, Canada. Can. J. Earth Sci. **17**: 996–1006. doi: 10.1139/e80-100.
Marchildon, C. 2007. Évolution spatio-temporelle des palses et des lithalses de la région des rivières Sheldrake et Nastapoka, côte est de la baie d'Hudson, Nunavik. M.Sc. thesis, Laval University, Department of Geography, Québec, Que., Canada. 101 pp.
Ménard, E., Allard, M., and Michaud, Y. 1998. Monitoring of ground surface temperature in various biophysical micro-environments near Umiujaq, Eastern Hudson Bay, Canada. *In* Proceedings of the 7th International Conference on Permafrost, Yellowknife, N.W.T., Canada, 23–27 June 1998. *Edited by* A.G. Lewkowicz and M. Allard. Centre d'études Nordiques, Université Laval, Québec, Que., Canada. pp. 723–729.
Myers-Smith, I.H., Forbes, B.C., Wilmking, M., Hallinger, M., Lantz, T., Blok, D., and Sass, U.G.W. 2011. Shrub expansion in tundra ecosystems: dynamics, impacts and research priorities. Environ. Res. Lett. **6**: 045509. doi: 10.1088/1748-9326/6/4/045509.

Myers-Smith, I.H., Hallinger, M., Wilmking, M., Blok, D., Sass-Klaassen, U., Rayback, S.A., Weijers, S., Trant, A., Tape, K.D., Naito, A.T., Wipf, S., Rixen, C., Dawes, M., Wheeler, J., Buchwal, A., Baittinger, C., Macias-Fauria, M., Forbes, B.C., Lévesque, E., Boulanger-Lapointe, N., Beil, I., Ravolainen, V., and Wilmking, M. 2015. Methods for measuring arctic and alpine shrub growth: a review. Earth Sci. Rev. **140**: 1–13. doi: 10.1016/j.earscirev.2014.10.004.

Osterkamp, T.E., and Romanovsky, V.E. 1999. Evidence for warming and thawing of discontinuous permafrost in Alaska. Perm. Periglac. Proc. **10**: 17–37. doi: 10.1002/(SICI)1099-1530(199901/03)10:1<17::AID-PPP303>3.0.CO;2-4.

Payette, S., and Gauthier, B. 1972. Les structures de végétation: interprétation géographique et écologique, classification et application. Nat. Can. **99**: 1–26.

Payette, S., Filion, L., Delwaide, A., and Bégin, C. 1989. Reconstruction of tree-line vegetation response to long-term climate change. Nature, **341**(6241): 429–432. doi: 10.1038/341429a0.

Payette, S., Delwaide, A., Caccianiga, M., and Beauchemin, M. 2004. Accelerated thawing of subarctic peatland permafrost over the last 50 years. Geophys. Res. Lett. **31**: L18208. doi: 10.1029/2004GL020358.

Pelletier, M. 2015. Geomorphological, ecological and thermal time phase of permafrost degradation, Tasiapik, Nunavik (Québec, Canada). M.Sc. thesis, Université Laval, Department of Geography, Québec, Que., Canada. 69 pp.

Provencher-Nolet, L., Bernier, M., and Lévesque, E. 2014. Quantification des changements récents à l'écotone forêt-toundra à partir de l'analyse numérique de photographies aériennes. Ecoscience, **21**(3–4): 419–433. doi: 10.2980/21-(3-4)-3715.

Roche, Y., and Allard, M. 1996. L'enneigement et la dynamique du pergélisol: l'exemple du détroit de Manitounuk, Québec nordique. Géogr. Phys. Quat. **50**(3): 377–393. doi: 10.7202/033107ar. PMID: 29683143.

Romanovsky, V.E., Drozdov, D.S., Oberman, N.G., Malkova, G.V., Kholodov, A.L., Marchenko, S.S., and Vasiliev, A.A. 2010. Thermal state of permafrost in Russia. Perm. Periglac. Proc. **21**(2): 136–155. doi: 10.1002/ppp.683.

Ropars, P., and Boudreau, S. 2012. Shrub expansion at the forest–tundra ecotone: spatial heterogeneity linked to local topography. Environ. Res. Lett. **7**: 015501. doi: 10.1088/1748-9326/7/1/015501.

Rowland, J.C., Jones, C.E., Altmann, G., Bryan, R., Crosby, B.T., Geernaert, G.L., Hinzman, L.D., Kane, D.L., Lawrence, D.M., Mancino, A., Marsh, P., McNamara, J.P., Romonovsky, R.E., Toniolo, H., Travis, B.J., Trochim, W., and Wilson, C.J. 2010. Arctic landscapes in transition: responses to thawing permafrost. EOS Trans. **91**: 229–230. doi: 10.1029/2010EO260001.

Schimel, J.P., Bilbrough, C., and Welker, J.M. 2004. Increased snow depth affects microbial activity and nitrogen mineralization in two Arctic tundra communities. Soil Biol. Biochem. **36**(2): 217–227. doi: 10.1016/j.soilbio.2003.09.008.

Schuur, E.A.G., McGuire, A.D., Schadel1, C., Grosse, G., Harden, J.W., Hayes, D.J., Hugelius, G., Koven, C.D., Kuhry, P., Lawrence, D.M., Natali, S.M., Olefeldt, D., Romanovsky, V.E., Schaefer, K., Turetsky, M.R., Treat, C.C., and Vonk, J.E. 2015. Climate change and the permafrost carbon feedback. Nature, **520**: 171–179. doi: 10.1038/nature14338. PMID: 25855454.

Seguin, M.K., and Allard, M. 1984. Le pergélisol et les processus thermokarstiques de la région de la rivière Nastapoca, Nouveau-Québec. Géogr. Phys. Quat. **38**: 11–25. doi: 10.7202/032532ar. PMID: 29683143.

Shevtsova, A., Haukioja, E., and Ojala, A. 1997. Growth response of subarctic dwarf shrubs, Empetrum nigrum and Vaccinium vitis-idaea, to manipulated environmental conditions and species removal. Oikos, **78**: 440–458. doi: 10.2307/3545606.

Sturm, M., Holgren, I.J., Konig, M., and Morris, K. 1997. The thermal conductivity of seasonal snow. J. Glaciol. **43**: 26–41. doi: 10.1017/S0022143000002781.

Sturm, M., Racine, C., and Tape, K. 2001. Climate change: increasing shrub abundance in the Arctic. Nature, **411**(6837): 546–547. doi: 10.1038/35079180. PMID: 11385559.

Sturm, M., Schimel, J., Michaelson, G., Welker, J.M., Oberauer, S.F., Liston, G.E., Fahnestock, J., and Romanovsky, V. 2005. Winter biological processes could help convert Arctic tundra to shrubland. BioScience, **55**: 17–26. doi: 10.1641/0006-3568(2005)055[0017:WBPCHC]2.0.CO;2.

Tarnocai, C., and Stolbovoy, V. 2006. Northern peatlands: their characteristics, development and sensitivity to climate change. *In* Peatlands: evolution and records of environmental and climate changes. Developments in Earth Surface Processes. *Edited by* I.P. Martini, A. Martinez Cortizas, and W. Chesworth. Elsevier, Amsterdam, the Netherlands. Vol. 9, pp. 17–51.

Tarnocai, C., Canadell, J.G., Schuur, E.A.G., Kuhry, P., Mazhitova, G., and Zimov, S. 2009. Soil organic carbon pools in the northern circumpolar permafrost region. Global Biogeochem. Cycles, **23**: GB2023. doi: 10.1029/2008GB003327.

Thibault, S., and Payette, S. 2009. Recent permafrost degradation in bogs of the James Bay area, northern Quebec, Canada. Perm. Periglac. Proc. **20**: 383–389. doi: 10.1002/ppp.660.

Thompson, C.C., McGuire, A.D., Clein, J.C., Chapin, F.S., III, and Beringer, J. 2006. Net carbon exchange across the Arctic tundra–boreal forest transition in Alaska 1981–2000. Mitig. Adapt. Strateg. Glob. Chang. **11**: 805–827. doi: 10.1007/s11027-005-9016-3.

Tremblay, B., Lévesque, E., and Boudreau, S. 2012. Recent expansion of erect shrubs in the low Arctic: evidence from Eastern Nunavik. Environ. Res. Lett. **7**: 035501. doi: 10.1088/1748-9326/7/3/035501.

Vincent, W.F., Lemay, M., and Allard, M. 2017. Arctic permafrost landscapes in transition: towards an integrated Earth system approach. Arct. Sci. **3**: 39–64. doi: 10.1139/as-2016-0027.

Walker, D.A., Epstein, H.E., Gould, W.A., Kelley, A.M., Kade, A.N., Knudson, J.A., and Shur, Y. 2004. Frost-boil ecosystems: complex interactions between landforms, soils, vegetation and climate. Perm. Periglac. Proc. **15**(2): 171–188. doi: 10.1002/ppp.487.

Zamin, T.J., and Grogan, P. 2012. Birch shrub growth in the low Arctic: the relative importance of experimental warming, enhanced nutrient availability, snow depth and caribou exclusion. Environ. Res. Lett. **7**: 034027. doi: 10.1088/1748-9326/7/3/034027.

Zhang, T., Osterkamp, T.E., and Stamnes, K. 1996. Influence of the depth hoar layer of the seasonal snow cover on the ground thermal regime. Water Resour. Res. **32**(7): 2075–2086. doi: 10.1029/96WR00996.